Cryogenics 72 (2015) 103–110

Contents lists available at ScienceDirect

Cryogenics

journal homepage: www.elsevier.com/locate/cryogenics

Numerical analysis of the two-phase heat transfer in the heat exchanger of a mixed refrigerant Joule–Thomson cryocooler

R.M. Damle [a], P.M. Ardhapurkar [b], M.D. Atrey [a,*]

[a] Refrigeration and Cryogenics Laboratory, Department of Mechanical Engineering, Indian Institute of Technology Bombay, Powai, Mumbai 400076, Maharashtra, India
[b] S.S.G.M. College of Engineering, Shegaon 444203, India

ARTICLE INFO

Article history:
Received 3 August 2015
Received in revised form 26 September 2015
Accepted 28 September 2015
Available online 8 October 2015

Keywords:
J–T cryocooler
Mixed-refrigerant
Heat-exchanger
Numerical

ABSTRACT

The recuperative heat exchanger is the most critical component of a mixed refrigerant Joule–Thomson cryocooler. The heat transfer process in such a heat exchanger takes place under two-phase conditions due to simultaneous boiling of the cold stream and condensation of the hot stream. This results in higher heat transfer coefficients as compared to single phase heat exchange. Moreover, depending on the composition of non-azeotropic mixtures, the boiling and condensation take place over a range of temperatures. In this work, the two-phase heat transfer in the recuperative heat exchanger of a mixed refrigerant Joule–Thomson cryocooler is studied. A numerical model is developed to simulate the heat transfer in a helically coiled tube-in-tube heat exchanger with nitrogen–hydrocarbons mixtures. The heat transfer coefficients for the two-phase flow under boiling and condensation are evaluated with the correlations available in the literature. The physical properties of the mixtures are evaluated at local conditions of temperature and pressure. The numerical results obtained with the developed model are compared with the experimental data reported in the literature. Additionally, the model predictions are also compared with new experimental data reported in the present work.

1. Introduction

One of the principle reasons of using a gas mixture (nitrogen and hydrocarbons) as a working fluid in Joule–Thomson (J–T) cryocoolers is the increase of efficiency as compared to nitrogen alone [1–4]. Moreover, for obtaining cryogenic temperatures, the operational pressures can be as low as 10–20 bar in comparison to the high pressures of around 200 bar with nitrogen as the working fluid. This is because, for mixtures, the heat transfer in the recuperative heat exchanger takes place in the liquid–vapour dome at subcritical pressures as the mixture components start boiling/condensing over intermediate temperatures. The two-phase flow also results in higher heat transfer coefficients as compared to pure gas. In addition, there are advantages of simple construction, fast cool down time and high reliability. Furthermore, by selecting appropriate mixture compositions, it is possible to reach temperatures in the range of 80–150 K which can be useful for various applications like cooling infrared sensors, cryosurgery, cryopreservation, gas chillers, etc.

Several researchers have reported numerical and experimental studies on mixed refrigerant Joule–Thomson (MR J–T) cryocoolers. Mostly, these studies [1–7] are focussed on the optimization of mixture compositions and thermodynamic performance of the overall refrigeration system. There are few studies in the literature related to performance analysis of heat exchanger. This is due to lack of general heat transfer model that allows realistic prediction of the flow boiling and condensation heat transfer coefficients for a multi-component fluid at cryogenic temperatures. Gong et al. [8] reported experimental data for different mixtures in terms of pressure drop and temperature profiles for a tubes-in-tube heat exchanger. Alexeev et al. [9] simulated tubes-in-tube heat exchanger with different mixtures. However, the numerical predictions are not compared with experimental data except for the pressure drop on the shell side. Ardhapurkar et al. [10] predicted the hot side temperatures with a simple energy balance equations for a multi tubes-in-tube heat exchanger without considering thermal losses and pressure drop in the heat exchanger. Nellis et al. [11] obtained experimental data for heat transfer coefficients for mixed refrigerants used in the cryocooler at various operating conditions.

Recently, Ardhapukar et al. [12] assessed the existing heat transfer correlations with the experimental data reported by Nellis et al. [11] for mixtures (nitrogen–hydrocarbons). They modified the Granryd correlation [13] for higher mass fluxes. Ardhapurkar et al. [14] carried out a performance analysis of the recuperative heat exchanger for a MR J–T cryocooler. Modified Granryd

* Corresponding author. Tel.: +91 (22)2576 7522; fax: +91 (22)2572 6875.
E-mail address: matrey@iitb.ac.in (M.D. Atrey).

http://dx.doi.org/10.1016/j.cryogenics.2015.09.010
0011-2275/

Nomenclature

A	cross-sectional area (m^2)
CV	control volume
Cp	specific heat (J/kg K)
d	characteristic dimension (m)
dx	CV length (m)
G	mass velocity (kg/m^2 s)
h	heat transfer coefficient (W/m^2 K)
H	enthalpy (J/kg)
k	thermal conductivity (W/m K)
L	length of the finned tube/external annulus (m)
l_p	wetted perimeter (m)
m	mass (kg)
$\dot{m}$	mass flow rate (kg/s)
$\dot{m}_f$	given mass flow rate (kg/s)
Nu	Nusselt number
Pr	Prandtl number
p	pressure (N/m^2)
Re	Reynolds number
T	temperature (K)
ΔT_{max}	maximum temperature difference (K)
ΔT_g	temperature glide (K)
V	velocity (m/s)
V_g	gas phase velocity (m/s)
V_l	liquid phase velocity (m/s)
X_{tt}	Martinelli parameter
x_g	gas mass fraction

Greek symbols

μ	viscosity (Ns/m^2)
ρ	density (kg/m^3)
τ_w	wall shear stress (N/m^2)

Subscripts

bub	bubble point
dew	dew point
c	cold gas in the external annulus
cond	condensation
eq	equivalent
g	gas
h	hot gas in the inner tube
in	inlet
l	liquid
lo	liquid only
m	mixture
out	outlet
w	tube wall
(–)	average over CV

correlation is used for boiling while the correlations of Shah [15], Dobson-Chato [16], and Cavallini-Zecchin [17] are employed for condensation. Based on the measured temperature profiles for different mixtures, the theoretically evaluated overall heat transfer coefficients agreed well with those obtained from LMTD method. Ardhapukar et al. [18] also conducted experiments on a MR J–T cryocooler with different nitrogen–hydrocarbons mixtures. They also reported the pressure drop and the temperature profiles along the length of the hot and cold sides of the heat exchanger. Baek et al. [19] reported experiments with argon-freon mixtures in a micro channel heat exchanger and concluded that the conventional two-phase heat transfer coefficient correlations can be used.

Although there are numerous experimental studies on MR J–T cryocoolers, numerical analysis of the recuperative heat exchanger in particular has received less attention in the literature. The recuperative heat exchanger is a very critical component of a J–T cryocooler and even more so for a MR J–T cryocooler. In a MR J–T cryocooler, boiling of the cold fluid stream and condensation of the hot fluid stream take place over a range of temperatures (known as the temperature glide). This temperature glide depends on the composition of the mixture. The two-phase heat transfer is accompanied with a large variation of physical properties and the heat transfer coefficients depend on the amount of liquid and gas phases given by the gas mass fraction (x_g). Moreover, the operating parameters like pressure and mass flow rates also govern the heat transfer characteristics. Therefore, the heat exchanger design plays a very important role in the performance of a MR J–T cryocooler in terms of the cooling capacity and the lowest attainable temperatures.

The objective of the present work is to develop a numerical model for simulating the two-phase heat transfer occurring in the recuperative heat exchanger of a MR J–T cryocooler. A numerical model can be used to optimize the mixture compositions and operating conditions (i.e., mass flow rates and pressure ratios) to obtain the desired cold temperatures. For this purpose, a helically coiled tube-in-tube heat exchanger is modelled in this work. For this heat exchanger, Ardhapurkar et al. [18] have reported the temperature profiles of the hot and the cold fluid streams for three different mixtures of nitrogen–hydrocarbons. The temperature profiles obtained with the developed numerical model are then compared with the experimental data [18]. Furthermore, experiments conducted on a different heat exchanger with two more mixtures are also reported in this work. This new heat exchanger has the same dimensions as those reported by Ardhapurkar et al. [18]. However, temperature profile of the hot fluid is not measured in this case. The temperature sensors are installed only on the cold side to measure cold fluid temperature profile. The present numerical model is also employed to predict the hot and cold fluid temperature profiles of this heat exchanger.

In this work, a one-dimensional steady state model is implemented for the resolution of the fluid streams and solid tubes with the control volume method. The flow boiling heat transfer coefficients are estimated with the modified Granryd correlation [12] while condensation heat transfer coefficients are obtained with the Cavallini and Zecchin [20] correlation. The frictional pressure drop is calculated assuming a homogeneous-flow model. The variation of the physical properties of the mixture, with temperature and pressure, along the heat exchanger length is taken into account. The physical properties are calculated from the aspenONE software [20]. Axial conduction along the tubes is also considered.

2. Numerical model

A one-dimensional steady model is developed for the simulation of the fluid streams and the solid tubes which together form the heat exchanger. The different elements of the heat exchanger are divided into a series of control volumes (CVs) over which the governing equations are solved. The control volume arrangement is shown in Fig. 1. A brief description of the numerical model is presented in this section.

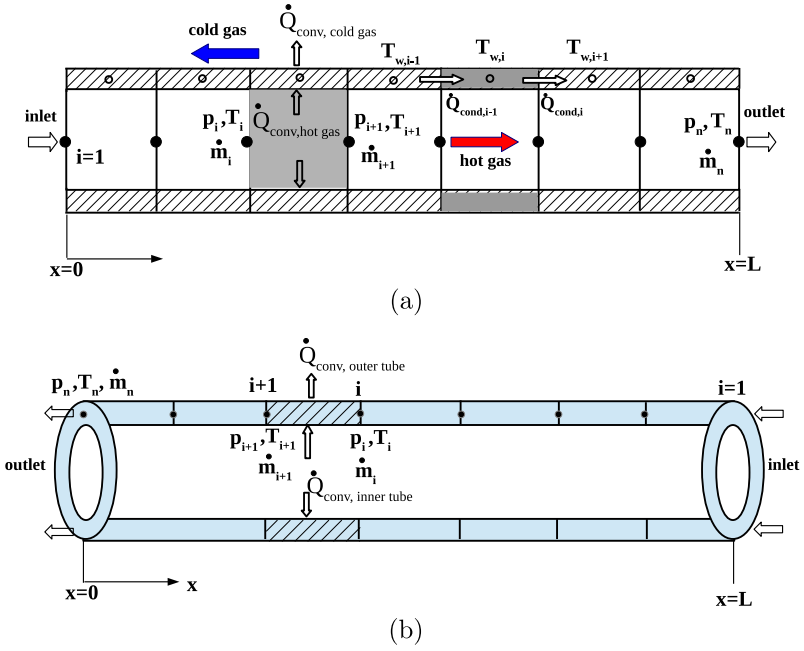

Fig. 1. CV arrangement: (a) inner fluid and inner tube; (b) outer fluid.

2.1. Assumptions

The assumptions made in the derivation of the governing equations are as follows :

(i) heat transfer and fluid flow along the heat exchanger length are considered to be one-dimensional and steady;
(ii) axial conduction in the fluid is neglected;
(iii) body forces and axial stresses are negligible;
(iv) inner and outer tubes are assumed to be adiabatic at ends;
(v) emissivity of the outer tube is constant and receives outside radiation at ambient temperature.
(vi) effect of helical coil on the heat transfer is neglected.
(vii) homogeneous model is employed for pressure drop along the heat exchanger length.

2.2. Governing equations

The basic equations of conservation of mass, momentum and energy for the fluid elements and energy conservation equation for solid elements are written in a differential form. The conservation of mass over a fluid CV is:

$$\frac{\partial \dot{m}}{\partial x} = 0 \tag{1}$$

The conservation of momentum is given by:

$$\frac{\partial(\dot{m}V)}{\partial x} = -\frac{\partial p}{\partial x}\cdot A - \tau_w l_p \tag{2}$$

The two-phase mixture velocity at a given cross-section is calculated as $V = x_g V_g + (1 - x_g)V_l$ and the shear stress is calculated with the homogeneous flow model.

The energy equation in terms of enthalpy is written as:

$$\frac{\partial(\dot{m}H)}{\partial x} = h \cdot l_p \cdot (T_w - \bar{T}) - \frac{\partial(\dot{m}V^2/2)}{\partial x} \tag{3}$$

A general energy equation for the solid elements is the following:

$$\frac{\partial}{\partial x}\left(kA\frac{\partial T}{\partial x}\right) + \dot{Q}_{conv} + \dot{Q}_{rad} = 0 \tag{4}$$

$\dot{Q}_{conv}$ represents the heat transfer per unit length due to convection from the surfaces of the solid elements. $\dot{Q}_{rad}$ is the heat transfer per unit length due to radiation considered only for the outer tube surface.

2.3. Boundary conditions

The inlet temperature, pressure and mass flow rate is known for both hot and cold fluid streams. The inner and outer solid tubes are assumed to be adiabatic at ends. Thus,

$$at\ x = 0 : \dot{m} = \dot{m}_f, \quad T = T_{h,in}, \quad p = p_{h,in}, \quad \frac{dT_w}{dx} = 0 \tag{5}$$

$$at\ x = L : \dot{m} = \dot{m}_f, \quad T = T_{c,in}, \quad p = p_{c,in}, \quad \frac{dT_w}{dx} = 0 \tag{6}$$

2.4. Heat transfer correlations

There are many correlations available for condensation and boiling in the literature. However, their validity with mixtures of nitrogen and hydrocarbons in the cryogenic range is not well established. Recently, Ardhapurkar et al. [12] assessed the existing boiling heat transfer correlations with the experimental data reported by Nellis et al. [13] for mixtures (nitrogen–hydrocarbons). They modified the Granryd correlation and recommended its use for flow boiling of mixtures at cryogenic temperatures which is given by:

$$h_m = h_{lo}\left(\frac{F_p}{1+A}\right) \tag{7}$$

where, h_{lo} is the liquid only heat transfer coefficient calculated from the Dittus–Boelter equation with properties of mixture as given below.

$$h_{lo} = 0.023\left(\frac{k_l}{d}\right)\left[(1-x_g)\frac{Gd}{\mu}\right]^{0.8} Pr_l^{0.4} \tag{8}$$

where, $Pr_l = \frac{\mu_l Cp_l}{k_l}$ is the liquid Prandtl number. F_p, the parameter for flow boiling of pure refrigerants, is given by:

$$F_p = 2.37\left(0.29 + \frac{1}{X_{tt}}\right)^{0.85} \tag{9}$$

X_{tt} is the Martinelli parameter for turbulent-liquid and turbulent-vapour flow calculated as:

$$X_{tt} = \left(\frac{1-x_g}{x_g}\right)^{0.9}\left(\frac{\rho_g}{\rho_l}\right)^{0.5}\left(\frac{\mu_l}{\mu_g}\right)^{0.1} \tag{10}$$

The parameter A in the above equation is:

$$A = \left(\frac{F_p}{C_{lg}}\right)x_g^2\left[\left(\frac{1-x_g}{x_g}\right)\left(\frac{\mu_g}{\mu_l}\right)\right]^{0.8}\left(\frac{Pr_l}{Pr_g}\right)^{0.4}\left(\frac{k_l}{k_g}\right)\left(\frac{Cp_g}{Cp_w}\right) \tag{11}$$

where C_{lg} is the enhancement factor to account for the gas and liquid interface effects. $C_{lg} = 2$ was recommended by Granryd [13] for evaporation of refrigerants. Ardhapurkar et al. [12], in the modified Granryd correlation, proposed $C_{lg} = 1.4$ for $G > 500$ kg/m^2 s. Cp_w is the apparent local specific heat for a non-azeotropic mixture and is defined as $Cp_w = \left(\frac{\partial H}{\partial T}\right)_p$.

Based on the conclusions drawn by Ardhapurkar et al. [14], the correlation of Cavallini and Zecchin [17] is employed for calculating the condensation heat transfer coefficients. Cavallini and Zecchin [17] correlation for condensation is a modified form of the well-known Dittus–Boelter correlation. This is given by:

$$h_{cond} = 0.05\left(\frac{k_l}{d}\right)Re_{eq}^{0.8} Pr_l^{1/3} \tag{12}$$

where Re_{eq} is the equivalent Reynolds number for two-phase flow and G_{eq} is the equivalent mass flux. These are given calculated according to:

$$Re_{eq} = \frac{G_{eq} d}{\mu_l} \tag{13}$$

$$G_{eq} = G\left((1-x_g) + x_g\left(\frac{\rho_l}{\rho_g}\right)^{0.5}\right) \tag{14}$$

The above condensation correlation is corrected with the Silver [21] and Bell and Ghaly [22] method to account for the non-isothermal condensation process of mixtures. The corrected heat transfer coefficient (h_m) is evaluated as:

$$\frac{1}{h_m} = \frac{1}{h_{cond}} + \frac{Z_g}{h_g} \tag{15}$$

Here, h_g is the vapour only heat transfer coefficient calculated with the Dittus–Boelter equation as:

$$h_g = 0.023\left(\frac{k_g}{d}\right)Re_g^{0.8} Pr_g^{0.4} \tag{16}$$

The parameter Z_g is the ratio of the sensible cooling of the vapour to the total cooling rate and is given by:

$$Z_g = x_g Cp_g \frac{dT_{dew}}{dH} \approx x_g Cp_g \frac{\Delta T_g}{\Delta H_m} \tag{17}$$

where Cp_g is the specific heat of gas phase and $\frac{dT_{dew}}{dH}$ is the slope of the dew point temperature curve with respect to mixture enthalpy. This is approximated by the ratio of temperature glide ΔT_g and ΔH_m is the enthalpy of isobaric condensation of the mixture.

2.5. Resolution of fluid and solid elements

For resolving the governing equations, the fluid streams are divided into a series of control volumes (CVS) along their length as shown earlier in Fig. 3. For both the hot and cold fluid streams, the variables (e.g. p, T, $\dot{m}$) are known at the inlet cross-section. Thus, an iterative step-by-step method is suitable here to obtain the variable values at subsequent cross-sections by marching in the flow direction. For the solid elements, integration of Eq. (4) over a CV results in a system of linear algebraic equations. TDMA (Tri-Diagonal Matrix Algorithm) method is used for solving this system of equations. The cases were run with two different grid sizes of 150 CVs and 300 CVs. It was observed that there were no significant difference in the profiles obtained with these grid sizes. The results reported in this work are with a grid size of 300 CVs along the heat exchanger length. Global iterations are made within a pseudo-transient procedure until the maximum increments of all the variables are below $1.0e^{-6}$ to obtain the steady state distributions.

3. Experimental set-up and heat exchanger configuration

The experimental set-up with the heat exchanger amongst other devices and instrumentation is shown in Fig. 2. The details of the experimental set-up and measurement of mass flow rates, temperatures and composition can be found in the work reported by Ardhapurkar et al. [18]. In the present work, experiments are carried out on the same set-up using heat exchanger without temperature sensors inside the inner tube. Fig. 3 shows the pictorial view of the helically coiled tube-in-tube heat exchanger. The length of the heat exchanger is 15 m. The overall height of the heat exchanger assembly shown in Fig. 3 is around 650 mm. Table 1 specifies the geometrical parameters of the heat exchanger.

Typically, the high pressure gas mixture enters the inner tube of the heat exchanger at a pressure in the range of 10–20 bar and at a temperature of around 300 K. The low pressure gas mixture flows through the external annulus at lower pressure of around 4–6 bar in the opposite direction. Its inlet temperature is dependent on the lowest temperature that can be attained with a given mixture composition and can be around 100–150 K. The high pressure stream condenses inside the inner tube while the low pressure stream evaporates in the external annulus. This forms a counter-flow heat exchanger with two-phase heat transfer.

4. Results and discussion

For comparing the numerical model with the experimental data, the tube-in-tube heat exchanger is simulated with three different mixtures (Mix#1, Mix#2 and Mix#3). The numerically obtained temperature profiles are compared with the experimental data reported by Ardhapurkar et al. [18] for these mixtures. It should be noted that the experiments [18] with Mix#1, Mix#2 and Mix#3 are carried out on a heat exchanger (HX-I) with temperature sensors on both hot and cold sides. Additionally, in the present work, experiments are conducted on a new heat exchanger (HX-II) with two more mixtures (Mix#4 and Mix#5). The experiments with HX-II are carried out on the same experimental set-up shown in the previous section. The heat exchanger (HX-II) has the same geometrical configuration as that of Ardhapurkar et al. [18] as specified in Table 1. However, unlike HX-I, the heat exchanger HX-II is not installed with temperature sensors for measuring the hot fluid temperature profile. In the experiments with HX-II, temperatures of the cold fluid are measured along the length of the heat exchanger. For the hot fluid, temperatures are measured only at the inlet and outlet of the heat exchanger. The developed

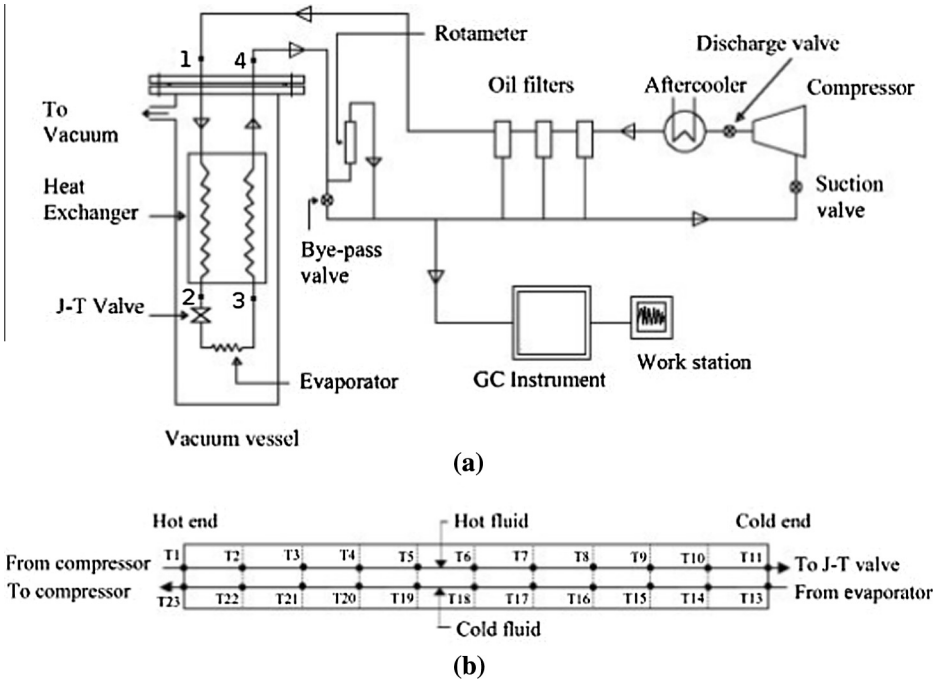

Fig. 2. Experimental set-up.

Fig. 3. Photograph of the heat exchanger.

Table 1
Dimensions of the recuperative heat exchanger.

Parameter	Size (mm)
Inner tube, ID (mm)	4.83
Inner tube, OD (mm)	6.35
Outer tube, ID (mm)	7.89
Outer tube, OD (mm)	9.52
Length of heat exchanger (m)	15
Coil diameter (mm)	200
Coil pitch (mm)	14.5
Number of turns	23

Table 2
Mixture compositions and lowest temperature ranges.

Mixture	Composition (% mol) ($N_2/CH_4/C_2H_6/C_3H_8/iC_4H_{10}$)	Temperature range (K)
Mix#1	5.5/42.5/36/5/11	140–150
Mix#2	36/15/13/19/17	<100
Mix#3	15.5/31/16.5/21/16	110–120
Mix#4	40.5/11/12.5/16.5/19.5	100–110
Mix#5	30.5/18/16/18.5/17	100–110

numerical model is also employed for predicting the temperature profiles in HX-II with Mix#4 and Mix#5.

The charged compositions for all the mixtures are specified in Table 2. Cases with Mix#1, Mix#2, Mix#3 and Mix#4 are simulated with their composition in circulation. However, for the case with Mix#5, the charged composition is employed for simulation as the composition in circulation could not be measured. The mixture compositions used in simulations are indicated in the corresponding captions of Figs. 4–8.

The thermo-physical properties and the boiling/condensation temperatures are evaluated by plotting the p-h diagram for each mixture using the aspenOne software [20] as reported by Ardhapurkar et al. [18]. The different constituents of the mixture have different boiling points and their relative percentages affect the temperature profiles of the hot and cold fluid streams. Propane (231 K) and iso-butane (260 K) are high boiling components, ethane is a middle boiling component (184 K), while nitrogen (77 K) and methane (111 K) are low boiling components. Therefore, the lowest temperature achievable with Mix#1 is between 140 and 150 K with high percentage of ethane than that of Mix#2 and Mix#3. Mix#2 and Mix#3 have almost similar percentages of

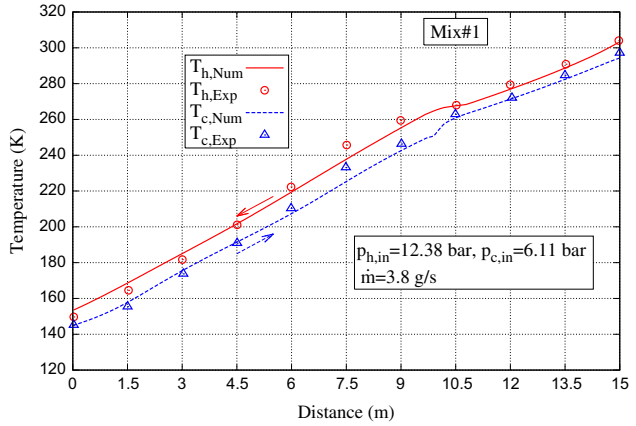

Fig. 4. Temperature profiles for Mix#1 (circulation composition: 6.99/46.335/33.533/3.996/9.146).

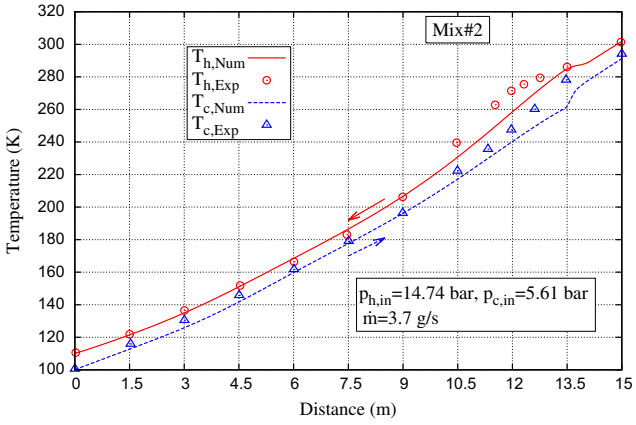

Fig. 5. Temperature profiles for Mix#2 (circulation composition: 39.86/16.865/12.845/17.38/13.045).

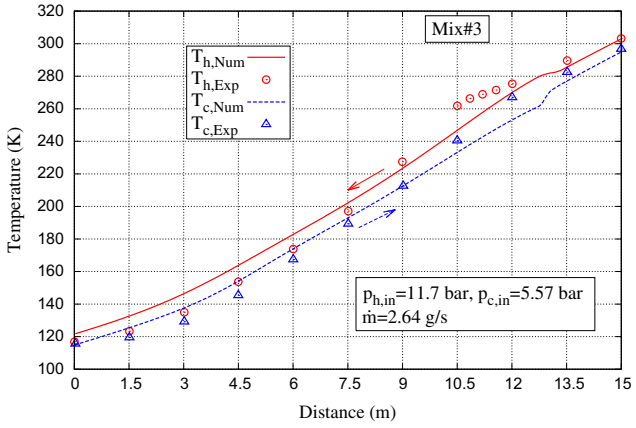

Fig. 6. Temperature profiles for Mix#3 (circulation composition: 18.455/32.785/16.05/20.14/12.57).

propane and iso-butane. The highest percentage of nitrogen in Mix#2 results in lowest temperatures less than 100 K. Mix#3 has three times more nitrogen and the almost 70% methane as compared to Mix#1 which leads to temperatures of around 110–120 K. Mix#4 also has high percentage of nitrogen as in Mix#2, but the lower percentage of methane keeps the lowest

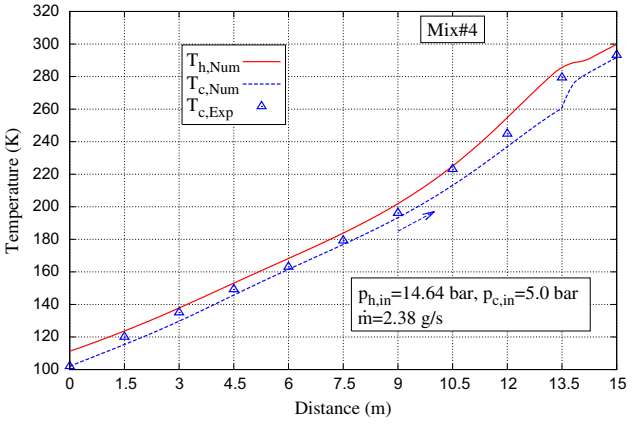

Fig. 7. Temperature profiles for Mix#4 (circulation composition: 47.63/11.26/9.68/16.77/14.66).

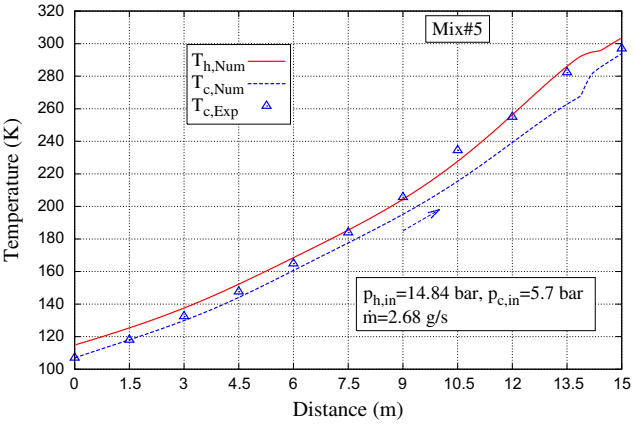

Fig. 8. Temperature profiles for Mix#5 (charged composition: 30.5/18/16/18.5/17).

temperature within 100–110 K. Finally, Mix#5 is a balanced mixture in terms of the percentages of hydrocarbons and moderate percentage of nitrogen. The lowest temperature for this mixture is also in the range of 100–110 K. Thus, it can be observed that the mixture composition is very important for reaching a given temperature range.

The operating parameters for all the cases simulated in this work are given in Table 3. This table gives the experimental values of mass flow rates, pressures and temperature at the inlet and outlet of the hot and cold sides of the heat exchanger. The location of the pressure measurements, shown in Table 3, are numbered in Fig. 2. $p_{h,in}$ and $p_{h,out}$, for the hot fluid stream, are measured at locations 1 and 2 respectively. For the cold fluid stream $p_{c,in}$ and $p_{c,out}$ are measured at locations 3 and 4 respectively. The numerical results obtained for different mixtures with their respective operating conditions are compared with the experimental data. Fig. 4 shows this comparison for the heat exchanger (HX-I) with Mix#1. The outlet temperatures of the hot and the cold fluids are 149.29 K and 296.89 K respectively. At these temperatures, the hot fluid leaves the heat exchanger in a two-phase state while the cold fluid leaves the heat exchanger in a single phase gas condition. This can be seen from the dew point (T_{dew}) and bubble point (T_{bub}) temperatures given in Table 4 for both the hot and the cold fluid streams at their respective mean pressures. The temperature glide (ΔT_g), difference between the dew point and bubble point temperature, is also given in Table 4.

It is observed from Fig. 4 that the temperature profiles of the hot and the cold fluid streams change significantly over the heat

Table 3
Operating parameters for different mixtures.

Mixture	T_{low} (K)	$\dot{m}$ (g/s)	$p_{h,in}$ (bar)	$T_{h,in}$ (K)	$p_{c,in}$ (bar)	$T_{c,in}$ (K)	$p_{h,out}$ (bar)	$p_{c,out}$ (bar)
Mix#1	143.98	3.80	12.38	303.18	6.11	144.87	11.41	3.2
Mix#2	98.62	3.70	14.74	301.50	5.61	100.17	13.95	2.6
Mix#3	113.45	2.64	11.70	302.66	5.57	114.83	11.01	2.3
Mix#4	102.00	2.38	14.64	299.49	5.00	102.08	14.44	2.0
Mix#5	106.36	2.68	14.84	303.22	5.70	107.00	14.60	2.2

Table 4
Temperature glide for different mixtures.

Mixture	Hot side temperatures (K)			Cold side temperatures (K)		
	T_{bub}	T_{dew}	ΔT_g	T_{bub}	T_{dew}	ΔT_g
Mix#1	139.29	267.64	128.35	114.62	245.46	130.84
Mix#2	103.61	287.15	183.54	86.74	253.77	167.03
Mix#3	110.97	281.79	170.82	92.42	253.56	161.14
Mix#4	101.78	289.39	187.60	84.01	251.55	167.55
Mix#5	104.67	295.26	190.58	86.13	258.31	172.18

exchanger length. These variations can be attributed to the variation of the specific heat of the hot and the cold streams with temperature [18]. Towards the gas phase region at the hot end, due to lower heat transfer coefficients and nearly equal heat capacities, the temperature profiles are linear with a constant temperature difference. At the interface of the single phase and two-phase regions, the specific heat of the condensing hot stream increases and that of the evaporating cold stream decreases. Therefore, the temperature difference between the streams increases suddenly with the corresponding change in slope of the two streams. Near the cold end, higher liquid fraction and in turn higher specific heat of the cold fluid cause decrease in the slope of the cold temperature profile.

The above observations are also reflected in the numerically predicted temperature profiles of the hot and the cold fluid streams. From Fig. 4 it is seen that the numerical values agree well with the experimental data in both the single phase and two-phase regions. The relative differences between the numerical and experimental values of temperature are less than 3.5%. The experimental and numerical values of maximum temperature difference (ΔT_{max}) between the hot and the cold streams are 13.14 K and 13.99 K respectively. The experimentally observed location of ΔT_{max} is at 9.0 m from the cold end while the same occurs at 9.89 m in case of numerical prediction. The qualitative variation of ΔT is also seen in the numerical predictions.

Figs. 5 and 6 show the numerically and experimentally obtained temperature profiles of the fluid streams for Mix#2 and Mix#3 respectively. In these cases, the rise in the temperature difference, similar to Mix#1, is seen at the interface of the single phase and two-phase regions. From the middle of the heat exchanger towards the cold end, the temperature profiles are linear with a constant temperature difference due to comparable specific heat of the fluid streams. At the cold end, higher specific heat of the hot stream causes deviation in the temperature profiles. Both these effects are reflected in the predicted temperature profiles. In case of Mix#3, the trends are similar to that of Mix#2. However, towards the cold end, between 0 and 3 m, the slope of the cold fluid temperature profile reduces drastically. This is because of the larger liquid fraction due to higher percentage of methane. Here again, the qualitative trends of the experimental observations are seen in the predicted temperature profiles.

For Mix#2, the numerical predictions are not so well for the region close to the gas phases. For Mix#3, towards the warm end of the heat exchanger, in the single phase and transition regions, the numerical predictions are on the lower side for both the hot and the cold streams. The predicted temperature profiles are on the higher side for the rest of the heat exchanger. For Mix#2 and Mix#3 the maximum relative differences of temperature are less than 6% and 8.5% respectively. The numerical and experimental values of ΔT_{max}, both around 23.9 K, agree well for Mix#2. However, the location of ΔT_{max} shifts towards the hot end by 1.45 m as compared to the experimental observation. For Mix#3 the experimental value of ΔT_{max} is 21.34 K and the numerical value is 18.28 K. In this case, the location of ΔT_{max} shifts 2.25 m when compared with the experimentally observed location.

One of the reasons for the observed differences is the temperature glide of the mixtures. The temperature glide is the difference between the dew point and bubble point temperature of the mixture and is dependent on the mixture composition. The temperature glides for all the mixtures are shown in Table 4. It can be observed that the temperature glide is lowest for Mix#1 (130.84 K) as compared to Mix#2 (167.03 K) and Mix#3 (161.14 K), while the temperature glides for mixtures Mix#2 and Mix#3 are of the same order. When the temperature glide is high, the mixture effect is larger and the deviations of the existing heat transfer correlations are large. Also, the physical property variation over the temperature range is more. Therefore, the differences between the numerical and the experimental results are higher for Mix#2 and Mix#3. Also, as compared to Mix#1, the shift in ΔT_{max} is higher for Mix#2 and Mix#3. The above observation conforms with the findings of Ardhapurkar et al. [12] wherein it was concluded that the predictions made with the modified Granryd correlation were influenced by the temperature glide of the mixture. They observed higher deviations, in predictions of temperature with respect to the experimental values, for mixtures with higher temperature glide.

Also, for the cold fluid, it is observed that the differences are more in the region close to single phase gas. These differences may be attributed to the significant changes of physical properties of the boiling fluid in this region. Moreover, the correlation is more accurate when the mass fraction x_g is in the range of 0.1–0.75 [12]. This explains the reason of these differences. A similar observation was reported by Ardhapurkar et al. [14], in their calculation (theoretical and experimental) of overall heat transfer coefficients with modified Granryd correlation on the boiling side and Cavallini and Zecchin [17] correlation for condensation. The deviations reported by them between the experimental and theoretical values of heat transfer coefficients were in the range of 3–18.7%.

Table 5 shows the comparison between the numerical and experimental values of outlet temperature on the hot and cold sides. In case of Mix#1, the relative differences in the outlet temperature of the hot and cold streams are below 3.0% while those for Mix#2 and Mix#3 are below 5%. Thus, the numerical predictions at the ends of the heat exchanger are in fair agreement with

Table 5
Comparison of outlet temperatures of the hot and cold fluid streams.

Mixture	$T_{h,out}$ (K)		$T_{c,out}$ (K)	
	Experimental	Numerical	Experimental	Numerical
Mix#1	149.29	153.587	296.89	294.292
%r.d		(2.87)		(0.87)
Mix#2	110.53	110.244	293.50	291.194
%r.d		(0.258)		(0.78)
Mix#3	116.26	121.801	296.16	294.904
%r.d		(4.76)		(0.42)
Mix#4	109.37	111.436	293.24	291.695
%r.d		(1.88)		(0.53)
Mix#5	111.01	115.36	296.91	293.84
%r.d		(3.92)		(1.03)

the measured values. This numerical model can therefore be used to estimate the overall two-phase heat transfer in the recuperative heat exchanger for mixtures of nitrogen–hydrocarbons.

Additionally, in the present work, experimental data for two more mixtures (Mix#4 and Mix#5) are reported. Experiments are carried out on a new heat exchanger (HX-II) with these mixtures. For this heat exchanger, only the cold side temperatures are measured along with the outlet temperatures on both hot and cold sides. In this heat exchanger there is no disturbance to the flow that can be caused by the hot side temperature sensors. However, Ardhapurkar et al. [18] did not observe significant differences in pressure drop and temperature profiles in the experiments made with and without sensors on the hot side of the heat exchanger. After comparing the numerical results with the experimental data [18], the developed model is employed for the simulation of the heat exchanger HX-II with these mixtures. Figs. 7 and 8 show the predicted temperature profiles of the hot and the cold fluid streams for Mix#4 and Mix#5 respectively. The measured values of temperature on the cold side are also plotted in these figures. The qualitative trends of these mixtures are similar to Mix#2 because of similar operating pressures and mixture compositions. The maximum relative differences of temperature are 6.6% for Mix#4 while the same for Mix#5 are 8.02%. These differences are mainly observed in the region where there is a change of phase in the heat exchanger as observed for mixtures 1–3. From Table 4 it can be seen that the temperature glide of the cold fluid for Mix#4 is similar to Mix#2. The temperature glide on the cold side is highest for Mix#5. Also, as mentioned earlier, Mix#5 is simulated with charged composition instead of the composition in circulation. Due to this reason, the numerically obtained cold side temperatures for Mix#4 agree with the experimental values to a better extent as compared to Mix#5. Apart from the change of phase region, the numerical values agree reasonably well with the experimental data. The values of the outlet temperatures for both mixtures are within 4% of the measured values as can be seen in Table 5. The numerical model presented in this work is thus able to capture the overall heat transfer in the heat exchanger for different mixture compositions and operating conditions.

5. Conclusions

Numerical analysis of the recuperative heat exchanger of a mixed refrigerant J–T cryocooler is presented in this paper. A one-dimensional steady state model has been developed for the simulation of the two-phase heat transfer. Physical property variation of the mixtures with temperature and pressure is taken into account along with axial conduction in the solid tubes. The heat transfer coefficients on the boiling side are calculated with the modified Granryd correlation and the correlation of Cavallini and Zecchin [20] is used to evaluate the condensation heat transfer.

The numerical model is firstly verified with the experimental data of Ardhapurkar et al. [18] for three different nitrogen–hydrocarbons mixtures. Additionally, experimental data for two more mixtures with a different heat exchanger is also reported. The numerically obtained temperature profiles of this new heat exchanger are also compared with the measured values. The maximum relative differences of temperature, between the experimental and numerical values, are less than 8%, and the relative differences of the outlet temperatures are below 5% for all the mixtures worked out in this study. Thus, the numerical predictions compare reasonably well with the experimental data.

It is observed that the differences are larger for mixtures with higher temperature glide and in the region close to the single phase gas region. However, the numerical model is able to estimate the overall two-phase heat transfer in the recuperative heat exchanger for mixtures of nitrogen–hydrocarbons. The qualitative trends of the temperature profiles of both hot and cold fluid streams are also captured by the developed model.

References

[1] Brodyanskii VM, Gromov EA, Grezin AK, Yagodin VM, Nikolaskii VA, Tashchina DG. Efficient throttling cryogenic refrigerators which operate on mixtures. Chem Petrol Eng 1971;7(12):1057–61.
[2] Longsworth RC, Boiarski MJ, Klusmier LA. 80 K closed cycle throttle refrigerator. Cryocoolers 1995;8:537–41.
[3] Walimbe NS, Narayankhedkar KG, Atrey MD. Experimental investigation on mixed refrigerant Joule–Thomson cryocooler with flammable and nonflammable refrigerant mixtures. Cryogenics 2010;50(10):653–9.
[4] Alexeev A, Haberstroh Ch, Quack H. Further development of a mixed gas Joule–Thomson refrigerator. Adv Cryog Eng 1998;43:1667–74.
[5] Keppler F, Nellis G, Klein SA. Optimization of the composition of a gas mixture in a Joule–Thomson cycle. HVACR Res 2004;10(2):213–30.
[6] Gong MQ, Luo EC, Zhou Y, Liang JT, Zhang L. Optimum composition calculation for multicomponent cryogenic mixture used in Joule–Thomson refrigerators. Adv Cryog Eng 2000;45:283–90.
[7] Lakshmi Narasimhan N, Venkatarathnam G. Effect of mixture composition and hardware on the performance of a single stage J–T refrigerator. Cryogenics 2011;251(8):446–51.
[8] Gong MQ, Wu JF, Luo EC, Qi YF, Hu QG, Zhou Y. Study on the overall heat transfer coefficient for the tube-in-tube heat exchanger used in mixed-gases coolers. Adv Cryog Eng 2002;47B:1483–90.
[9] Alexeev A, Thiel A, Haberstroh Ch, Quack Q. Study of behavior in the heat exchanger of a mixed gas Joule–Thomson cooler. Adv Cryog Eng 2000;45:307–14.
[10] Ardhapurkar PM, Sridharan A, Atrey M. Investigations on two-phase heat exchanger for mixed refrigerant Joule–Thomson cryocooler. Adv Cryog Eng 2012;57A:706–13.
[11] Nellis G, Hughes C, Pfotenhauer J. Heat transfer coefficient measurements for mixed gas working fluids at cryogenic temperatures. Cryogenics 2005;45(8):546–56.
[12] Ardhapurkar PM, Sridharan A, Atrey M. Flow boiling heat transfer coefficients at cryogenic temperatures for multi-component refrigerant mixtures of nitrogen–hydrocarbons. Cryogenics 2014;59:84–92.
[13] Granryd E. Heat transfer in flow evaporation of non-azeotropic refrigerant mixtures – a theoretical approach. In: Proc. 18th int congress of refrigeration, Montreal. vol. 3; 1991. p. 1330–4.
[14] Ardhapurkar PM, Sridharan A, Atrey M. Performance evaluation of heat exchanger for mixed refrigerant J–T cryocooler. Cryogenics 2014;63:49–56.
[15] Shah MM. A general correlation for heat transfer during film condensation inside pipes. Int J Heat Mass Transfer 1979;22:547–56.
[16] Dobson MK, Chato JC. Condensation in smooth horizontal tubes. J Heat Transfer Trans ASME 1998;120:193–213.
[17] Cavallini A, Zecchin R. A dimensionless correlation for heat transfer in forced convection condensation. In: Proceedings of the 6th int heat transfer conference, Tokoyo. vol. 3; 1974. p. 309–13.
[18] Ardhapurkar PM, Sridharan A, Atrey M. Experimental investigation on temperature profile and pressure drop in two-phase heat exchanger for mixed refrigerant Joule–Thomson cryocooler. Appl Therm Eng 2014;66:94–103.
[19] Baek S, Lee C, Jeong S. Investigation of two-phase heat transfer coefficients of argon-freon cryogenic mixed refrigerants. Cryogenics 2014;64:29–39.
[20] aspenONE V 7.1. Aspen Technology Inc, Burlington, MA 01803, USA; 2009.
[21] Silver L. Gas cooling with aqueous condensation. Trans Inst Chem Eng 1947;25:30–42.
[22] Bell KJ, Ghaly MA. An approximate generalized design method for multicomponent/partial condenser. AIChE Symp Ser 1973;69:72–9.